DOTATOC PET/CT imaging of a typical carcinoid tumor in a human ex-vivo perfused lung lobe

Alexis Slama[1,2]^, Benedikt M. Schaarschmidt[3], Özlem Okumus[1,2], Ken Herrmann[4], Clemens Aigner[1,5], Stephane Collaud[1,2]#, Hubertus Hautzel[4]#

[1]Department of Thoracic Surgery, University Medicine Essen, Ruhrlandklinik, Essen, Germany; [2]Department of Thoracic Surgery, Cologne-Merheim Medical Centre, Witten/Herdecke University, Cologne, Germany; [3]Department of Diagnostic and Interventional Radiology, University Hospital Essen, Essen, Germany; [4]Department of Nuclear Medicine, University Medicine Essen, Essen, Germany; [5]Department of Thoracic Surgery, Medical University of Vienna, Vienna, Austria

#These authors contributed equally to this work.

Correspondence to: Dr. Alexis Slama. Krankenhaus Köln-Merheim, Department of Thoracic Surgery, Cologne-Merheim Medical Centre, Ostmerheimer Str. 200, 51109 Cologne, Germany. Email: SlamaA@kliniken-koeln.de

Abstract: The use of Isolated lung perfusion (ILP), combined with medical imaging modalities such as positron emission tomography-computed tomography (PET/CT), provides real-time visualization of tumors in ventilated and perfused vital lung tissue. This experiment intends to show the feasibility and benefits of using ILP combined with PET/CT imaging. Following lung surgery on a 49-year-old male, his left lower lobectomy specimen, which held a typical carcinoid tumor, was preserved on normothermic ILP. Gallium-68-Edotreotide ([68Ga]-DOTATOC) was administered into the ILP circuit, and dynamic emission data from PET/CT was acquired. ILP was carried out for 120 minutes. Near physiologic gas exchange and glucose metabolism were preserved throughout the experiment. The time activity curves (TAC) of 5 different volumes of interest (VOI) showed notable differences in tracer uptake over time. The peripheral area of the carcinoid exhibited delayed but high somatostatin receptor agonist uptake compared to the surrounding parenchyma and the intrapulmonary artery. However, the central area of the carcinoid showed very low [68Ga]-DOTATOC uptake. This experiment demonstrates the potential of ILP combined with PET/CT for kinetic modeling in experimental nuclear medicine imaging. By providing visualization of tracer uptake in perfused lung tissue, this model could potentially improve our understanding of tumor physiology and molecular imaging

Keywords: Isolated lung perfusion; DOTATOC; neuroendocrine tumor (NET); positron emission tomography-computed tomography (PET/CT)

Introduction

In neuroendocrine tumors, somatostatin receptor imaging which is crucial for the diagnosis of distant metastases, is traditionally performed using Indium-111 [111In] diethylene-triamine-pentaacetate (DTPA) scintigraphy or Gallium-68 [68Ga] dodecane tetraacetic acid DOTA-peptide somatostatin receptor imaging (SSRI) with positron emission tomography (PET) (1). The introduction of hybrid imaging modalities into clinical practice, such as

---

^ ORCID: 0000-0002-0651-0832.
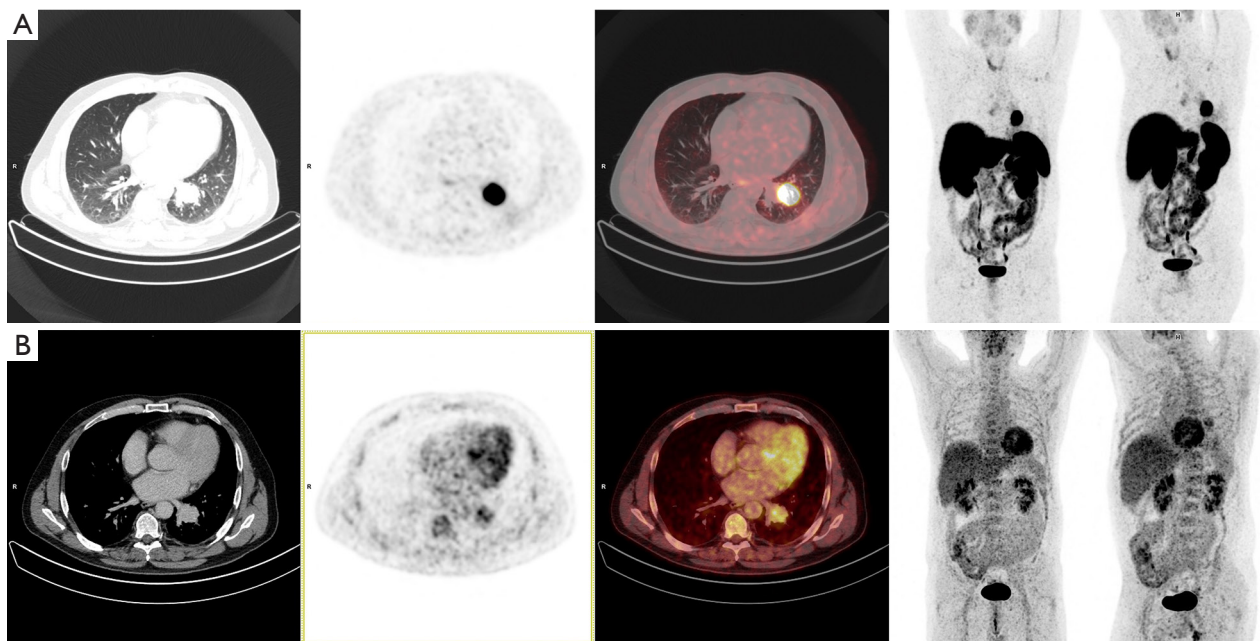
Figure 1 Preoperative PET/CT imaging. (A) Gallium-68-Edotreotide [68Ga]-DOTATOC PET/CT. (B) [18F]-FDG-PET/CT. To improve visualization of the FDG uptake of the carcinoid located dorsally of the heart, maximum intensity projections (MIP) are shown in anterior and left anterior oblique views. PET/CT, positron emission tomography-computed tomography; [68Ga]-DOTATOC, Gallium-68-Edotreotide; [18F]-FDG, fluorine-18-fluorodeoxyglucose.

combined PET/computed tomography scan (PET/CT) (2,3) and combined PET/magnetic resonance imaging (PET/MRI) (4,5), has promoted the use of [68Ga]-DOTA-peptide imaging by combining morphological imaging with the sensitivity of PET. [68Ga]-DOTA-peptide PET/CT and PET/MRI have become irreplaceable for initial tumor staging, patient selection for peptide receptor radionuclide therapy (PRRT), assessment of tumor response following chemotherapy, and liver-directed therapy (1,6). Recent approaches, such as the characterization of tumors through textural features in morphological imaging and PET, hold great potential regarding tumor response prediction and non-invasive grading of neuroendocrine tumors and neuroendocrine carcinomas, respectively (7-10). However, imaging features' relationship with histopathology requires further study before widespread clinical use. Isolated lung perfusion (ILP) (11,12) could be used to correlate histopathology with imaging in a viable organ without compromising patient safety and comfort. This brief report discusses our initial experience with *ex-vivo* ILP as a research tool in nuclear medicine imaging.

Methods

The study was conducted in accordance with the Declaration of Helsinki (as revised in 2013). Approval of this study was given by the ethics committee of the University of Duisburg-Essen (No. 17-7802_1-BO), and informed consent was obtained from the patient.

A 49-year-old male presented to our clinic with recurrent hemoptysis. The CT showed a suspicious 3.4 cm nodule in the left lower lobe with post-obstructive atelectasis. Subsequent fluorine-18 [18F]-fluorodeoxyglucose (FDG) PET/CT showed [18F]-FDG activity in the primary tumor (SUV_{max} 5.7) without evidence of distant metastasis (*Figure 1A*). Histopathology and immunohistochemistry identified a typical carcinoid (Ki67<1%) without nodal involvement. A [68Ga]-DOTATOC PET/CT showed intense and homogeneous somatostatin receptor 2 (SSTR2) expression in the primary tumor (SUV_{max} 32.1) (*Figure 1B*). The clinical tumor stage was cT2a cN0 cM0, stage IIA. Given the patients' good pulmonary function, a left lower lobectomy with lymph node dissection was performed.
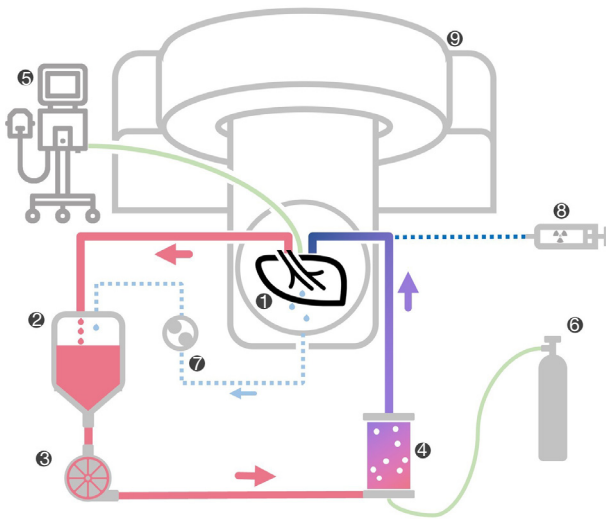
Figure 2 Schematic drawing of the experimental setting. The lung lobe [1] is placed on the PET/CT [9] gantry. Pulmonary venous perfusate flow is directed through a reservoir [2], a centrifugal pump [3], and a gas exchange membrane [4] before being pumped into the pulmonary artery. A ventilator [5] and a deoxygenation gas mixture [6] allow for physiological gas exchange. Green lines mark ventilation/gas tubes. An additional roller pump [7] collects leaked perfusate. [68Ga]-DOTATOC [8] was administered via the pulmonary artery. PET/CT, positron emission tomography-computed tomography; [68Ga]-DOTATOC, Gallium-68-Edotreotide.

Pathologic examination of the surgical specimen confirmed a pT2a pN0 (0/9) L0 V0 G1 R0 (stage IIA) typical carcinoid. The patient's recovery was uneventful, and no recurrence was seen on follow-up.

Isolated lung perfusion

Cold static preservation and ILP were performed according to our institutional protocol (11,12). After surgical retrieval of the lobe, the vasculature was flushed with cold preservation solution (1,000 mL Perfadex Plus®, 5,000 IU Heparin). The delay from intraoperative arterial clamping to cold static preservation was 15 min. The lobe was inflated via the bronchus, and vascular cannulas were sutured in. Cold ischemia was maintained for 343 min (5.7 hours) before perfusion. After gradual rewarming (37 ℃), the lobe was ventilated with 140 mL tidal volume (8 breaths/minute, FiO_2: 0.4, PEEP: 7 cmH$_2$O). Maximum perfusion flow was 610 mL/min, and the perfusate was

continuously deoxygenated. The circuit is depicted in *Figure 2*.

DOTATOC PET-CT imaging

The lung lobe was placed in a digital PET/CT (Vereos, Philips, The Netherlands) equipped with a 64-slice CT, time-of-flight technology, and an axial field-of-view of 17 cm. One gantry position covered the entire specimen. Forty minutes after the onset of ILP, data acquisition was started. After a high-resolution CT scan (100 kV, 250 mA, spatial resolution 0.67 mm × 0.67 mm), 100 MBq [68Ga]-DOTATOC was injected as a slow bolus via a long extension line into the pulmonary artery. The bolus reached the specimen 55 minutes after initiation of ILP. PET data were acquired in list mode for 80 min. The emission data was attenuation corrected, sorted into 60s-timeframes, and reconstructed with an iterative OSEM algorithm (3 iterations, 9 subsets) with a spatial resolution of 1 mm × 1 mm× 1 mm. Thereafter, spherical volumes-of-interest (VOI) (6 mm × 6 mm × 6 mm) were placed over the cannula (VOI1), a large intrapulmonary artery (VOI2), the center of the carcinoid (VOI3a), the periphery of the carcinoid (VOI3b), and the lung parenchyma (VOI4) (*Figure 3*). The mean count rates per ml in these VOIs were corrected for half-life, and finally used to derive VOI-based time activity curves (TAC), presented in *Figure 4*.

During ILP, strict safety precautions were taken.

Results

ILP was carried out for 120 minutes. Perfusate gas analysis of the venous outflow showed a final pO_2 of 94.2 mmHg and a pCO_2 of 42.4 mmHg (at t120 min). Regarding metabolic activity of the isolated lobe, glucose consumption was calculated to be 9.66 mg/min (linear regression analyses, R^2=0.8359) and lactate production 93.2 μmol/min (R^2=0.9717). There were no changes in electrolytic composition (cNa$^+$ 162 mmol/L; cK$^+$ 3.2 mmol/L; cCa^{2+} 0.61 mmol/L).

VOI1-TAC revealed a fast peak in the synthetic silicone cannula with a subsequent linear decrease. The count rates of the intrapulmonary artery (VOI2) increased less and plateaued after 20 min. Since the carcinoid tumor presented as a centrally hypometabolic lesion with an increased receptor expression in its periphery, two VOIs were defined. While the center VOI3a showed a low uptake, even less than the normal lung parenchyma, VOI3b placed
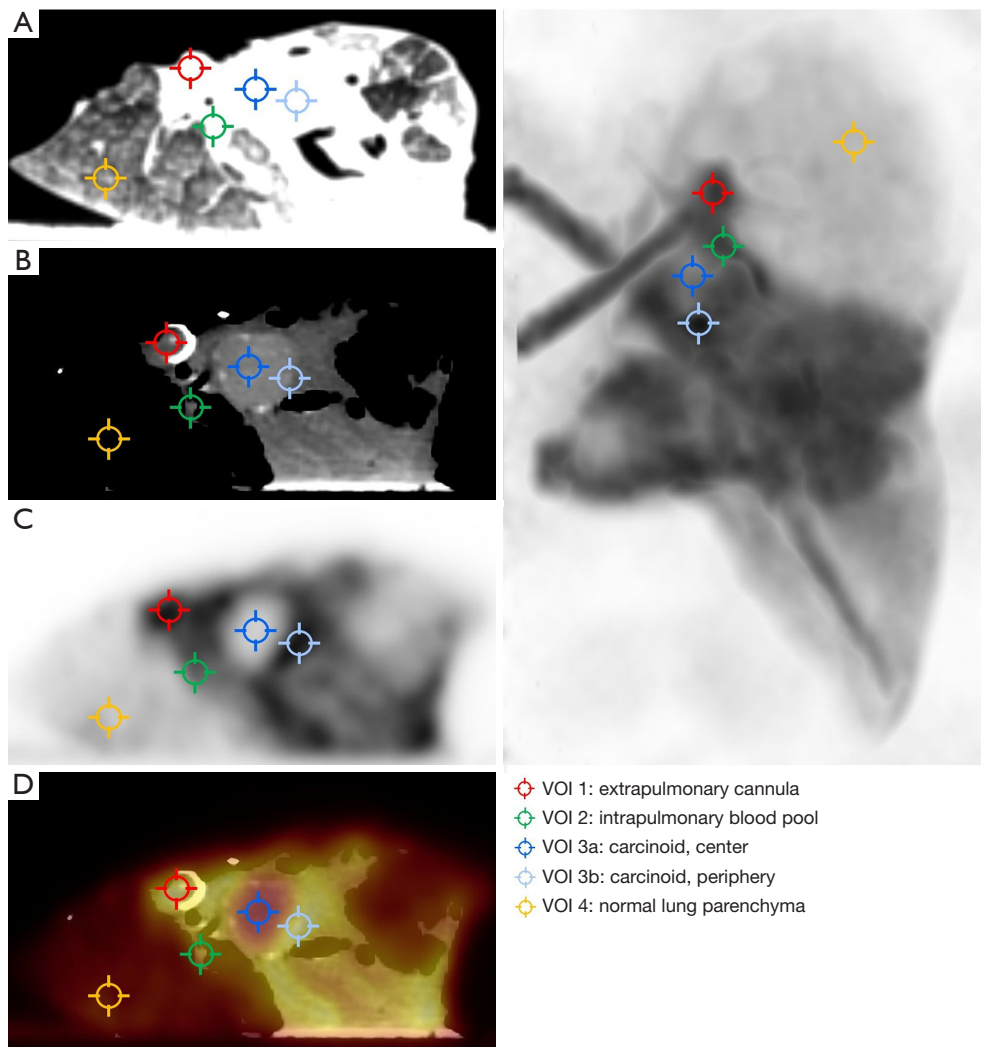
Figure 3 Defined volumes of interest in a transversal plane. (A) Lung window in computed tomography. (B) Mediastinal window. (C) PET image. (D) Fused PET/CT; right panel: multiplanar projection of PET images in coronal view. VOI, volume of interest; PET, positron emission tomography.
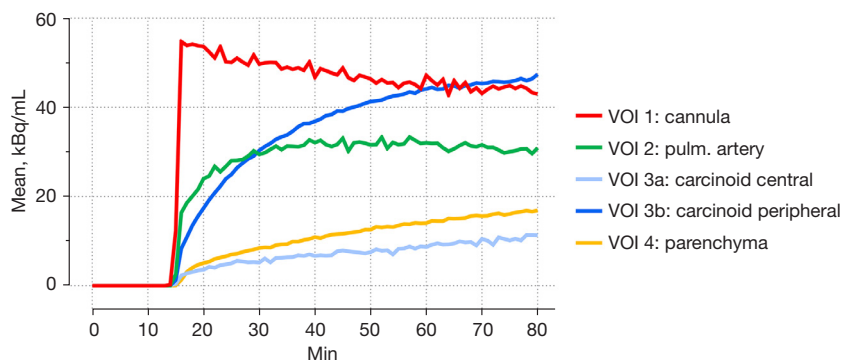
Figure 4 Count rates over time (from the start of data acquisition) in different VOI. The [68Ga]-DOTATOC slow bolus reached the surgical specimen 15 min after data acquisition was started. [68Ga]-DOTATOC, Gallium-68-Edotreotide; VOI, volumes of interest.

at the periphery of the typical carcinoid demonstrated an asymptotic rise with an activity concentration higher than in surrounding parenchyma (VOI4). Additionally, 15 min post-injection, tracer concentration in VOI3b exceeded that of the blood pool (VOI2). After that, the signal-to-background ratio of the tumor's periphery (VOI3b) to the blood pool (VOI2) increased to reach a plateau of 1.5 about 60 min post-injection. The TAC of the normal lung parenchyma (VOI4) constantly rose with an initial sigmoid course and linearly after that. The signal-to-background ratio of the carcinoid's periphery (VOI3b) to normal lung parenchyma (VOI4) peaked at 3.7 and linearly decreased to 2.8 at the end of the measurement.

Discussion

Typical carcinoids are low-grade pulmonary neuroendocrine tumors (NET) with low mitotic rates (13). Compared to other neuroendocrine tumors, they usually express SSTR2, making them suitable for imaging with [68Ga]-DOTA-peptides (14-16). Here, we present [68Ga]-DOTATOC PET/CT imaging of a typical human carcinoid in an *ex vivo* isolated lung lobe. This experiment demonstrates the feasibility of imaging perfusion and metabolism of extracorporeal organs over two hours with the possibility of acquiring TACs from afferent vessels for modeling input functions and from various regions within the respective organ. In our setting, five VOIs were defined to describe the tracer influx and circulating tracer in a pulmonary lobe artery, the unspecific SSTR2 uptake into normal lung parenchyma, and tumoral uptake in central and peripheral areas of the carcinoid.

Interestingly, after the arrival of the slow tracer bolus at the input cannula, a rapid increase of the TAC suggests an adherence of the tracer to the tubing, which might be attributable to the lipophilic properties of the silicone. This activity slowly decreased, suggesting that the tubing acts as a tracer reservoir with a continuous release. This effect might be considered a limitation of the experimental setup in its current form, especially when aiming for data modeling with a single bolus input and recirculation of the perfusate. In the lung parenchyma, count rates demonstrated a sigmoidal increase followed by a linear [68Ga]-DOTATOC uptake, probably due to the constant tracer supply.

In the carcinoid itself, we found two metabolically different areas. Contrary to the *in-vivo* observations, the center of the tumor appeared to be largely inactive, indicating a deficient expression of active receptor sites.

This difference might suggest early metabolic changes like internalization of the binding sites or degradation of the receptor, initiating central necrosis of the carcinoid due to changes in the peritumoral environment after resection. Another mechanism might be a switch in the binding of the intracellular SSTR2 part from GTP to GDP, making it inaccessible for SST receptor agonists like [68Ga]-DOTATOC (17). These hypothesized changes seem to precede alterations detectable by histopathology since there was no visible tumor necrosis on the final pathological report. In contrast, the tumor's periphery intensely accumulated [68Ga]-DOTATOC over time, suggesting viable tissue.

While kinetic measurements for dosimetry of the whole body and organ radiation exposure in patients undergoing [68Ga]-DOTATOC PET/CT are well established, data on [68Ga]-DOTATOC tumoral uptake and kinetics are sparse (18). Velikyan *et al.* performed dynamic PET/CT scans in three NET patients over 32 min. They added a static image at 50 min, which equals nearly equivalent observation time compared to the data presented here (19). However, only one of these patients was not treated with somatostatin analogues. In that patient, the NET uptake curve was very similar to our findings in the periphery TAC of the carcinoid, with an initial exponential rise followed by a slowly linear increase. Later, this intratumoral uptake pattern was replicated in another series (20). Our *ex vivo* [68Ga]-DOTATOC TAC in a viable NET lesion matches those *in vivo* data reports, emphasizing the isolated lung perfusion model's validity in molecular imaging.

Conclusions

Given our results of a centrally located SSTR2-reduction, which appeared to precede histological tumor alterations towards necrosis while in the carcinoid's periphery, the receptors remained preserved, this *ex vivo* ILP model might be beneficial for studying early metabolic effects on tumor-related micro-environmental changes. In addition, future applications of this model in PET/CT might include additional dynamic and interventional studies, e.g., pharmacological challenges. This brief report provides the basis for further research endeavors in this field.

Acknowledgments

Footnote

Conflicts of Interest: All authors have completed the ICMJE uniform disclosure form (available at https://qims.amegroups.com/article/view/10.21037/qims-22-1188/coif). AS reports that the article processing charges were covered by the Open Access Publication Fund of the University of Duisburg-Essen. The other authors have no conflicts of interest to declare.

Ethical Statement: The authors are accountable for all aspects of the work in ensuring that questions related to the accuracy or integrity of any part of the work are appropriately investigated and resolved. The study was conducted in accordance with the Declaration of Helsinki (as revised in 2013). Approval of this study was given by the ethics committee of the University of Duisburg-Essen (No. 17-7802_1-BO), and informed consent was obtained from the patient.

Open Access Statement: This is an Open Access article distributed in accordance with the Creative Commons Attribution-NonCommercial-NoDerivs 4.0 International License (CC BY-NC-ND 4.0), which permits the non-commercial replication and distribution of the article with the strict proviso that no changes or edits are made and the original work is properly cited (including links to both the formal publication through the relevant DOI and the license). See: https://creativecommons.org/licenses/by-nc-nd/4.0/.

References

1. Baudin E, Caplin M, Garcia-Carbonero R, Fazio N, Ferolla P, Filosso PL, Frilling A, de Herder WW, Hörsch D, Knigge U, Korse CM, Lim E, Lombard-Bohas C, Pavel M, Scoazec JY, Sundin A, Berruti A; ESMO Guidelines Committee. Electronic address: clinicalguidelines@esmo. Lung and thymic carcinoids: ESMO Clinical Practice Guidelines for diagnosis, treatment and follow-up( ). Ann Oncol 2021;32:439-51.
2. Antoch G, Saoudi N, Kuehl H, Dahmen G, Mueller SP, Beyer T, Bockisch A, Debatin JF, Freudenberg LS. Accuracy of whole-body dual-modality fluorine-18-2-fluoro-2-deoxy-D-glucose positron emission tomography and computed tomography (FDG-PET/CT) for tumor staging in solid tumors: comparison with CT and PET. J Clin Oncol 2004;22:4357-68.
3. Antoch G, Vogt FM, Freudenberg LS, Nazaradeh F, Goehde SC, Barkhausen J, Dahmen G, Bockisch A, Debatin JF, Ruehm SG. Whole-body dual-modality PET/CT and whole-body MRI for tumor staging in oncology. JAMA 2003;290:3199-206.
4. Heusch P, Nensa F, Schaarschmidt B, Sivanesapillai R, Beiderwellen K, Gomez B, Köhler J, Reis H, Ruhlmann V, Buchbender C. Diagnostic accuracy of whole-body PET/MRI and whole-body PET/CT for TNM staging in oncology. Eur J Nucl Med Mol Imaging 2015;42:42-8.
5. Martin O, Schaarschmidt BM, Kirchner J, Suntharalingam S, Grueneisen J, Demircioglu A, Heusch P, Quick HH, Forsting M, Antoch G, Herrmann K, Umutlu L. PET/MRI Versus PET/CT for Whole-Body Staging: Results from a Single-Center Observational Study on 1,003 Sequential Examinations. J Nucl Med 2020;61:1131-6.
6. Schaarschmidt BM, Wildgruber M, Kloeckner R, Nie J, Steinle V, Braat AJAT, Lohoefer F, Kim HS, Lahner H, Weber M, Theysohn J. (90)Y Radioembolization in the Treatment of Neuroendocrine Neoplasms: Results of an International Multicenter Retrospective Study. J Nucl Med 2022;63:679-85.
7. Weber M, Kessler L, Schaarschmidt B, Fendler WP, Lahner H, Antoch G, Umutlu L, Herrmann K, Rischpler C. Textural analysis of hybrid DOTATOC-PET/MRI and its association with histological grading in patients with liver metastases from neuroendocrine tumors. Nucl Med Commun 2020;41:363-9.
8. Weber M, Kessler L, Schaarschmidt B, Fendler WP, Lahner H, Antoch G, Umutlu L, Herrmann K, Rischpler C. Treatment-related changes in neuroendocrine tumors as assessed by textural features derived from (68)Ga-DOTATOC PET/MRI with simultaneous acquisition of apparent diffusion coefficient. BMC Cancer 2020;20:326.
9. Öksüz MÖ, Winter L, Pfannenberg C, Reischl G, Müssig K, Bares R, Dittmann H. Peptide receptor radionuclide therapy of neuroendocrine tumors with (90)Y-DOTATOC: is treatment response predictable by pre-therapeutic uptake of (68)Ga-DOTATOC? Diagn Interv Imaging 2014;95:289-300.
10. Werner RA, Ilhan H, Lehner S, Papp L, Zsótér N, Schatka I, Muegge DO, Javadi MS, Higuchi T, Buck AK, Bartenstein P, Bengel F, Essler M, Lapa C, Bundschuh RA. Pre-therapy Somatostatin Receptor-Based Heterogeneity Predicts Overall Survival in Pancreatic Neuroendocrine Tumor Patients Undergoing Peptide Receptor Radionuclide Therapy. Mol Imaging Biol 2019;21:582-90.

11. Schaarschmidt BM, Slama A, Collaud S, Okumus Ö, Steinberg H, Bauer S, Schildhaus HU, Theysohn J, Aigner C. Reversible occlusion of the pulmonary vasculature by transarterial embolisation with degradable starch microspheres: preclinical assessment in a human isolated lung perfusion model. Eur Radiol Exp 2022;6:6.

12. Slama A, Raber C, Hedderich C, Stockhammer P, Hegedüs B, Koch A, Theegarten D, Ploenes T, Aigner C. Implementation of an experimental isolated lung perfusion model on surgically resected human lobes. Sci Rep 2019;9:12193.

13. Pelosi G, Rindi G, Travis WD, Papotti M. Ki-67 antigen in lung neuroendocrine tumors: unraveling a role in clinical practice. J Thorac Oncol 2014;9:273-84.

14. Lococo F, Cesario A, Paci M, Filice A, Versari A, Rapicetta C, Ricchetti T, Sgarbi G, Alifano M, Cavazza A, Treglia G. PET/CT assessment of neuroendocrine tumors of the lung with special emphasis on bronchial carcinoids. Tumour Biol 2014;35:8369-77.

15. Deleu AL, Laenen A, Decaluwe H, Weynand B, Dooms C, De Wever W, Jentjens S, Goffin K, Vansteenkiste J, Van Laere K, De Leyn P, Nackaerts K, Deroose CM. Value of [(68)Ga]Ga-somatostatin receptor PET/CT in the grading of pulmonary neuroendocrine (carcinoid) tumours and the detection of disseminated disease: single-centre pathology-based analysis and review of the literature. EJNMMI Res 2022;12:28.

16. Venkitaraman B, Karunanithi S, Kumar A, Khilnani GC, Kumar R. Role of 68Ga-DOTATOC PET/CT in initial evaluation of patients with suspected bronchopulmonary carcinoid. Eur J Nucl Med Mol Imaging 2014;41:856-64.

17. Fani M, Mansi R, Nicolas GP, Wild D. Radiolabeled Somatostatin Analogs-A Continuously Evolving Class of Radiopharmaceuticals. Cancers (Basel) 2022.

18. Hartmann H, Zophel K, Freudenberg R, Oehme L, Andreeff M, Wunderlich G, Eisenhofer G, Kotzerke J. Radiation exposure of patients during 68Ga-DOTATOC PET/CT examinations. Nuklearmedizin 2009;48:201-7.

19. Velikyan I, Sundin A, Eriksson B, Lundqvist H, Sorensen J, Bergstrom M, Langstrom B. In vivo binding of [68Ga]-DOTATOC to somatostatin receptors in neuroendocrine tumours--impact of peptide mass. Nucl Med Biol 2010;37:265-75.

20. Velikyan I, Sundin A, Sörensen J, Lubberink M, Sandström M, Garske-Román U, Lundqvist H, Granberg D, Eriksson B. Quantitative and qualitative intrapatient comparison of 68Ga-DOTATOC and 68Ga-DOTATATE: net uptake rate for accurate quantification. J Nucl Med 2014;55:204-10.

DuEPublico

Duisburg-Essen Publications online